Melt depth and time variations during pulsed laser thermal annealing with one and more pulses

M. Hackenberg[1, *], M. Rommel[1],
M. Rumler[1], J. Lorenz[1], P. Pichler[1, 2]
[1]Fraunhofer IISB, Erlangen, Germany
[2]Chair of Electron Devices, University of Erlangen-Nuremberg, Erlangen, Germany
*Moritz.Hackenberg@iisb.fraunhofer.de

K. Huet[3], R. Negru[3], G. Fisicaro[4], A. La Magna[4],
N. Taleb[5], M. Quillec[5]
[3]Excico, Gennevilliers, France
[4]CNR IMM, Catania, Italy
[5]Probion, Bagneux, France

***Abstract*—In this work we present transient reflectivity measurements, maximum melt depths, and surface topographies of ion implanted silicon samples after pulsed excimer laser thermal annealing in the melting regime. The samples were annealed with different laser energies and number of pulses. We found that the melt dynamics change after the first laser pulse resulting in a shorter melt time but deeper melt depth. This can be explained by a change in reflectivity due to boron activation, surface modifications and small changes in the oxide thickness.**

I. INDTRODUCTION

Pulsed excimer Laser Thermal Annealing (LTA) is a process that allows dopant activation and damage removal for ion implanted silicon samples. The low thermal budget of a laser pulse with pulse duration in the nanosecond regime allows melting and recrystallization (due to liquid phase epitaxy) of the implanted region while no significant annealing of areas away from the irradiated surface [1] takes place. This process can, in general, be used for shallow junction formation and 3D integration. Devices using this process can, among others, be CMOS image sensors [2] or IGBTs [3].

While many publications focus on dopant redistribution and activation, e.g. [4, 5], the understanding of the thermal part of the process was less extensively investigated. However, knowledge about the thermal process and its fluctuations is important to predict the melting depth and temperatures inside the substrate and, finally, the properties of devices.

As the in-situ measurement of melt depth or temperatures inside the substrate is only possible with dedicated structures [6, 7] we conducted experiments measuring the melt time and melt depth to calibrate a simulation model with this data. For the calibration we only used the reflectivity of solid and liquid silicon as fitting parameters as they might change with sample preparation and process conditions. After calibration, this model is then able to predict the temperature inside the sample.

II. EXPERIMENTAL PROCEDURE AND RESULTS

Samples implanted with boron with an energy of 3 keV and a dose of $4 \cdot 10^{14}$ cm^{-2} as well as samples implanted with an energy of 30 keV and a dose of $1 \cdot 10^{15}$ cm^{-2} were anneled with 1, 3, 5 or 10 consecutive laser pulses of a XeCl excimer laser with a wavelength of 308 nm and a pulse duration of ~160 ns (FWHM). The time between the pulses was 0.5 s. Due to the low thermal budget, this is sufficient to cool the samples down to room temperature before being annealed with the next pulse. The samples implanted with 3 keV were annealed with pulses of 1.5 J/cm^2, 2.0 J/cm^2, 2.3 J/cm^2, and 2.6 J/cm^2. The samples implanted with 30 keV were annealed with pulses of 1.5 J/cm^2, 2.3 J/cm^2, 2.6 J/cm^2, and 2.9 J/cm^2. While 1.5 J/cm^2 is expected to be below the melt threshold, all other energy densities are expected to melt the surface.

During the laser irradiation, the melt time was monitored by transient reflectivity measurements (TRM), which means that the reflected intensity from a low energy continuous wave laser diode with a wavelength of 635 nm was monitored. Once the surface is molten, the solid-liquid interface penetrates further into the silicon which increases the reflectivity. Therefore, the measured intensity increases and finally saturates when the melt depth is around 20 nm [8]. The result of the measurements of this high-reflectivity time (t_{high}), which is the time for which the melt depth is at least 20 nm, is shown in Fig. 1. As no difference between the samples implanted with 3 keV and 30 keV was observed in terms of high-reflectivity time, we do not distinguish between these two cases. However, a difference betweeen the samples annealed with one and multiple pulses can be observed. After the first pulse, the high-reflectivity time decreases. Both the times for annealings for the first and consecutive pulses can be fitted by the function

$$t_{high} = B0 + B1 \cdot E_{las} + B2 \cdot E_{las}^2 \qquad (1)$$

This is the post-print version of the original article published in the proceedings of the ESSDERC 2013 conference, pp. 214-217,
which can be found at IEEEXplore (http://dx.doi.org/10.1109/ESSDERC.2013.6818857)

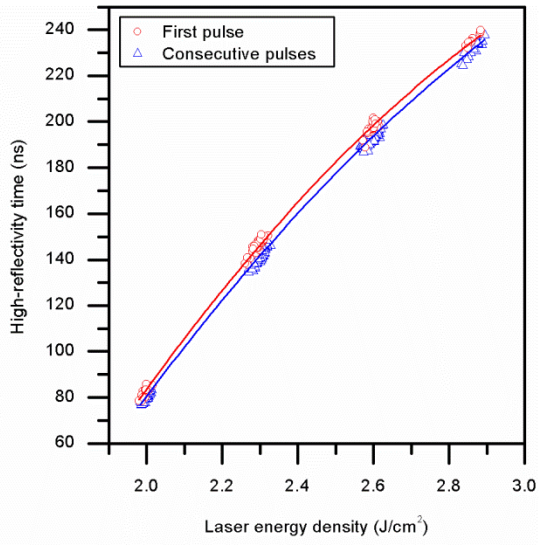

Figure 1: Measured high-reflectivity times for the first and consecutive laser pulses. The lines show the results of the fitting using (1) and parameters given in Table I.

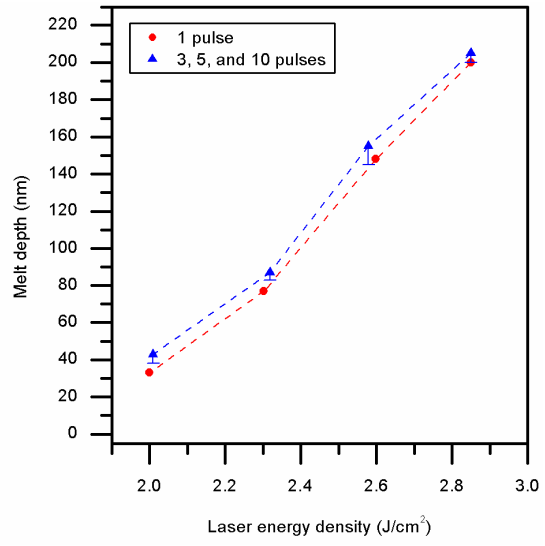

Figure 2: Extracted melt depths after the first and the consecutive laser pulses. The dotted lines are to guide the eye and the error bars in the curve for the melt depths of more than one pulse represent the spreading of the measurements after 3, 5, and 10 pulses.

TABLE I. PARAMETERS FOR (1) TO DESCRIBE THE HIGH REFLECTIVITY TIME AS FUNCTION OF THE LASER PULSE ENERGY DENSITY.

Number of pulses	*B0 (ns)*	*B1 (ns cm² J⁻¹)*	*B2 (ns cm⁴ J⁻²)*
First pulse	-617.73	472.98	-61.178
Consecutive pulses	-566.79	427.45	-51.90

with E_{las} denoting the energy density of the laser pulse. The parameters *B0*, *B1*, and *B2* found to describe t_{high} as a function of E_{las} for the first or a consecutive pulse are summarized in Table I.

The spreading of the high-reflectivity time is an indication of the pulse-to-pulse variation in energy density and pulse shape of this process. Both were measured in situ by a calorimeter and a photo diode. The pulse shape is characterized by the pulse duration (FWHM). It was measured to vary between 158 ns and 164 ns. The energy density was measured to vary by ± 1.5 % of the nominal energy density. Only for the nominal energy of 2.9 J/cm^2 larger deviations can be observed. In this case, deviations between -0.17% and -2.3% of the nominal energy density were measured.

As the melt depths cannot be extracted from the SIMS profiles directly, they were obtained by simulating the boron profiles with the model introduced in [4]. The resulting depths as function of the laser energy density are shown in Fig. 2. For the profiles annealed with more laser pulses, the energy density of the pulse resulting in the highest melt depth during simulation is given. As for the high-reflectivity time, two branches are visible. The annealing with only one pulse results in lower melt depths than samples annealed with more pulses. This is less surprising than in the case of the high-reflectivity time as during annealing with multiple pulses the pulse-to-pulse variations more probably lead to higher melt depths.

The surface topography of one sample of each annealing condition was investigated by atomic force microscopy (AFM) on 5 µm × 5 µm large areas. To describe the surface roughness, the root mean square average of height deviations from the mean plane R_q, defined by

$$R_q = \sqrt{(\sum_i^N Z_i^2)/N} \qquad (2)$$

is calculated with Z_i denoting the height deviation from the mean plane measured at position i and N the number of measured points.

For all measurements, the value of R_q is between 0.14 nm and 0.37 nm. No systematic difference in terms of R_q, like an increasing roughness with the number of laser pulses, pulse energy, or differences between the two implantation conditions, can be observed. Fig. 3 and 4 show the measured height maps of samples implanted with 30 keV and annealed with 1, 3, 5, and 10 laser pulses with 1.5 J/cm^2 and 2.6 J/cm^2. Two different kinds of surface texture can be seen. All samples annealed with 2.6 J/cm^2 show a wavy surface texture. The samples annealed with 1.5 J/cm^2 and 1, 3, and 5 pulses show a more homogenous surface texture instead. The sample annealed with 1.5 J/cm^2 and 10 pulses shows the wavy surface texture again. This wavy texture seems typical for samples for which the surface was molten, as all other samples (not shown) annealed with laser energy densities expected to melt the surface show it and all samples implanted with 3 keV annealed with 1.5 J/cm^2 (not shown) exhibit the more homogenous texture. This indicates and the simulations corroborated, that the surface of the sample implanted with 30 keV and annealed with 10 pulses of 1.5 J/cm^2 was molten at least during one of the pulses, which could be possible due to pulse variations, as the energy is close to the melting threshold.

III. SIMULATION AND DISCUSSION

The trends of the melt depth and melt duration during the first and the consecutive pulses are surprising. While the melt duration decreases after the first laser pulse, the melt depth

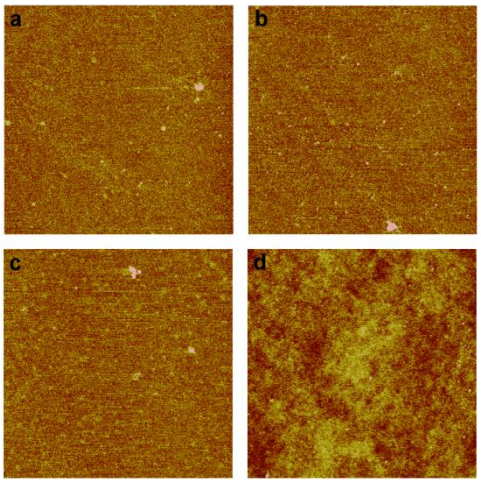

Figure 3: Surface topography measured by AFM on 5 µm times 5 µm of samples boron implanted with 30 keV. (a) 1 × 1.5 J/cm^2, (b) 3 × 1.5 J/cm^2 (c) 5 × 1.5 J/cm^2, and (d) 10 × 1.5 J/cm^2. The height scale goes from -1 nm (dark) to + 1 nm (bright) around the average height plane.

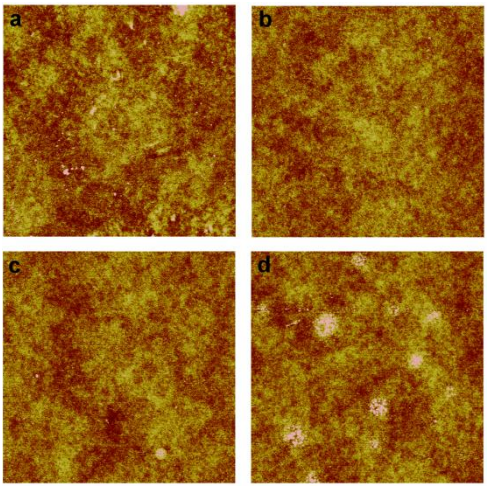

Figure 4: Surface topography measured by AFM on 5 µm times 5 µm of samples boron implanted with 30 keV. (a) 1 × 2.6 J/cm^2, (b) 3 × 2.6 J/cm^2 (c) 5 × 2.6 J/cm^2, and (d) 10 × 2.6 J/cm^2. The height scale goes from -1 nm (dark) to + 1 nm (bright) around the average height plane.

increases. Therefore, the complete process of melting and solidification is accelerated after the sample was molten for the first time. Furthermore, to achieve larger melt depths more energy needs to be absorbed in the silicon, as this is the only way to increase the melt depth as the physical properties like density, melting temperature, latent heat of melting or heat conduction are not expected to change.

The main difference between the samples appears to be the fact that all consecutive pulses but not the first pulse were applied to surfaces which were molten before. After ion implantation and laser annealing without melting, the surface of the samples is optically smooth as the width of the waviness is below the wavelength of the incident light. After melting, the width of the waviness is larger than 308 nm. This could change the optical properties, but the waviness height is only 2 nm. Therefore, the influence of the surface on the optical properties is expected to be small. Another possible reason could be the activation of the boron atoms [9] which leads to compressive strain. Furthermore, an SiO_x layer could form or dissolve during the process resulting in changed optical properties.

To test if a change in reflectivity could be the reason for the different behavior after melting, we used a simulation model for melting laser annealing [10] and adopted it to our experimental results by using the solid and liquid reflectivity as fitting parameter. The material parameters used for the simulation, except the reflectivity, are summarized in Table II. For the solid phase reflectivity R_{sol}, we used the temperature-dependent expression given by Unamuno and Fograrassy [11] of

$$R_{sol} = R_s + 4{\cdot}10^{-5}{\cdot}T/\mathrm{K} \qquad (3)$$

with $R_s = 0.59$ as starting point. For liquid silicon we started with the expression given by Černý et al. [11] of

$$R_{liq} = R_l + 9{\cdot}10^{-5}{\cdot}(T/\mathrm{K} - 1687) \qquad (4)$$

with $R_l = 0.67$. During the fitting, we only changed R_s and R_l in (3) und (4) as we assumed that this part should be dependent on the sample surface but not the temperature dependency.

The resulting reflectivity values are summarized in Table III. Fig. 5 shows a comparison of the measured and simulated high-reflectivity times for different measured pulse durations and energy densities. Fig. 6 shows a comparison of the measured and simulated melt depths using the measured energy densities and pulse durations for simulation. While in both cases some discrepancies between experiment and simulation remain, the trends are well reproduced. The melt duration after the first pulse decreases while the melt depth increases. This can be explained by two effects. First, slightly more energy is absorbed in the liquid phase for the case of more than one pulse. Second, the melting in that case starts later, allowing the heat to penetrate deeper into the substrate. Therefore, the melt front proceeds through a slightly preheated surface layer allowing a higher melt-in velocity.

The change of reflectivity can be explained by a change of oxide quality after melting, which would affect the reflectivity of the solid and liquid phase. In addition, the boron activation and the change in surface topography after melting affect the solid phase reflectivity only.

TABLE II. MATERIAL PROPERTIES USED FOR THE SIMULATION.

Material property	***Solid***	***Liquid***
Density (g cm^{-3})	2.32 [11]	2.52 [11]
Heat capacity (J kg^{-1} K^{-1})	Extracted from Fig.7 in [13]	1000 J kg^{-1} K^{-1} [11]
Latent heat (J cm^{-3})	4200 [13]	
Melting temperature (K)	1687 [14]	
Thermal conductivity (W cm^{-1} K^{-1})	T<1200K: $1526.3{\cdot}T^{-1.226}$ T>1200K: $9.0{\cdot}T^{-0.502}$ [11]	$0.502+(T-1687){\cdot}2.93{\cdot}10^{-4}$ [11]
Absorbtivity (cm^{-1})	$1.8{\cdot}10^6$ [11]	$1.9{\cdot}10^6$ [15]

TABLE III. REFLECTIVITY VALUES OBTAINED BY FITTING OF THE SIMULATION TO THE EXPERIMENTAL DATA.

Material property	R_s	R_l
1 pulse	0.494	0.789
2-10 pulses	0.535	0.785

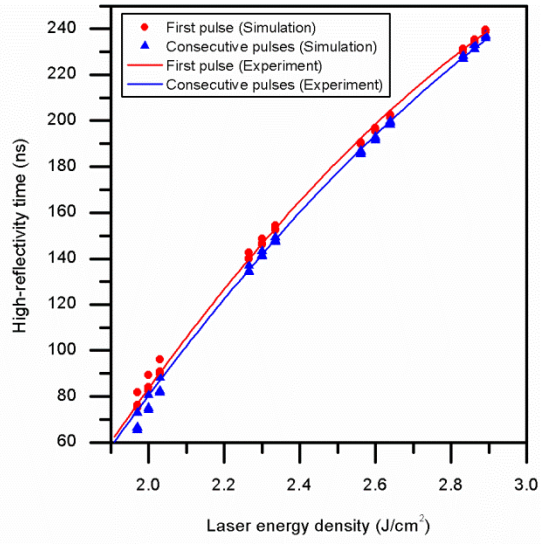

Figure 5: Simulated high-reflectivity times for different energy densities and pulse durations of 158 ns, 160 ns, 162 ns, and 164 ns (not specifically indicated), causing the spreading in the high-reflectivity times compared to the experimental data described by (1).

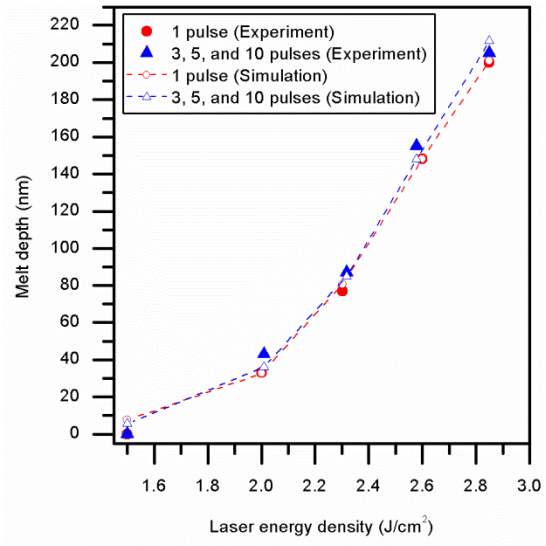

Figure 6: Simulated melt depth compared to the melt depth extracted from experiments for different laser energy densities. The dotted lines are to guide the eye only.

IV. CONCLUSION

We investigated the melt depths and melt durations of pulsed LTA with different energy densities and numbers of pulses. We found, that the samples behave different after they were molten for the first time. The melt duration decreases while the melt depth increases compared to the samples that were annealed for the first time.

Changing the reflectivity of solid and liquid silicon, our simulations could reproduce this trend. As a large change in the solid phase reflectivity but only a small change in the liquid phase reflectivity is necessary to explain it, the two branches could be a result of the change of diffraction index after boron activation and the change of the surface topography. The change in oxide quality or thickness is expected to be small, as it would also influence the liquid phase reflectivity, which changes only slightly.

ACKNOWLEDGMENT

The research leading to these results has received funding from the European Union Seventh Framework Programme (FP7/2007-2013) under grant agreement n° 258547 (ATEMOX). We thank M. Begel und P. Schuh for their help with the AFM measurements.

REFERENCES

[1] J. M. Poate and James W. Mayer, Laser annealing of semiconductors, Academic Press., 1982

[2] K. Huet, C. Boniface, J.Venturini, Z. Ait Fqir Ali-Guerry, R. Beneyton et al., "High performance and high yield junction formation with full device exposure lser thermal annealing, International Image sensor workshop, R12", 2011

[3] T. Gutt, H. Schulze, "Deep melt activation using laser thermal annealing for IGBT thin wafer technology", Proceedings of the 22nd international symposium on power semiconductor devices & ICs, pp. 29–32, 2010

[4] M. Hackenberg, P. Pichler, K. Huet, R. Negru, J. Venturini et al., "Modeling boron profiles in silicon after pulsedexcimer laser annealing", Proceedings of the 19th international conference on ion implantation technology, pp. 241–244, 2012

[5] G. Fisicaro, M. Italia, V. Privitera, G. Piccitto, K. Huet et al., "Solid phase phosphorous activation in implanted silicon by excimer laser irradiation", J. Appl. Phys, vol. 109, pp. 113513 – 113519, 2011

[6] M. O. thompson, J. W. Mayer, A. G. Cullis, H. C.Webber, N. G. Chew et al. "Silicon melt, regrowth, and amorphization velocities during pulsed laser irradiation", Phys. Rev. Lett., vol. 50, pp. 896- 899, 1983

[7] J. A. Kittle, P. G. Sanders, M. J. Aziz, D. P. Brunco, and M. O. Thompson, "Complete experimental test of kinetic models for rapid alloy solidification", Acta mater., vol 48, pp. 4797–4811, 2000

[8] M. Hermandez, J. Venturini, D. Zahorski, J. Boulmer, D. Débarre et al., "Laser thermal processing for ultra shallow junction formation: numerical simulation and comparison with experiment", Appl. Surf. Sci., vol. 208–209, pp. 345–351, 2003

[9] G. E. Jellison, Jr., S. P. Withrow, J. W. McCamy, J. D. Budai, D. Lubben et al., "Optical functions of ion-implanted, laser-annealed heavily doped silicon", Phys. Rev. B., vol. 52, pp. 14602–14614

[10] M. Hackenberg, P. Pichler, K. Huet, R. Negru, J. Venturini et al., "Enthalpy based modeling of pulsed excimer laser annealing for process simulation", Appl. Surf. Sci., vol. 258, pp. 9347–9351, 2012

[11] S. De Unamuno and E. Fogarassy, "A thermal description of the melting of c- and a-silicon under pulsed excimer lasers", Appl. Surf. Sci., vol 36, pp. 1–11, 1989

[12] R. Černý, P. Přikryl, K. M. A. El-Kader, V.Cháb, "Determination of the reflectivity of liquid semiconductors over a wide temperature range", Int. J. Thermophys., vol. 16, pp. 841–849, 1995

[13] P. D. Desai, "Thermodynamic properties of iron and silicon", J. Phys. Chem. Data, vol. 15, pp. 967– 983, 1986

[14] J. C. Brice, M. R. Brozel, "Melting points of Si", in Properties of crystaline silicon, R.Hull, INSPECT, 1999, pp. 155–157

[15] M. S. K. Fuchs, "Optical properties of liquid silicon: the integral equation approach", J. Phys.: Condens. Matter, vol. 12, pp. 4341–4351, 2000